EURASIAN PHYSICAL TECHNICAL JOURNAL

2025, Volume 22, No.2 (52)

https://doi.org/10.31489/2025N2/133-146

Received: 05/09/2024 Revised: 24/03/2025 Accepted: 11/04/2025 Published online: 30/06/2025

Original Research Article

UDC 523.44

SPECTROPHOTOMETRIC STUDIES OF ASTEROIDS I: REFLECTANCE SPECTRA

AimanovaG.K. [1*], Serebryanskiy A.V. [1], Shcherbina M.P. [2,3], Krugov M.A.[1]

[1] Fesenkov Astrophysical Institute, Almaty, Kazakhstan
[2] Institute of Astronomy of the Russian Academy of Sciences, Moscow, Russia
[3] Sternberg Astronomical Institute, Moscow State University, Moscow, Russia
*Corresponding author: gauhar@fai.kz

Abstract. *The paper presents the results of the analysis of the reflectivity spectra of asteroids based on observations obtained on 2024-02-22, 2023-11-03, 2023-11-04 and 2023-11-21 at the Assy-Turgen Observatory (77°.87114 E, 43°.225527 N, 2658 meters above sea level, international observatory code 217) using a long-slit spectrograph based on volume-phase holographic gratings (VPHG) installed at the prime focus of the AZT-20 telescope with an aperture of 1.5 meters. The observations were carried out in the low-resolution mode (R=600) in the range of 3500-7500Å using a grating of 360 lines per mm, a dispersion of 4.25Å per pixel, in the first binning in the EMCCD mode with a gain of 5 and an exposure time of 10 seconds, the slit width of 9 arc seconds. The spectrum of asteroids was measured using the differential method: by comparing the fluxes from the object and a standard star. Solar analog stars (G-class stars) were used as standards. Processing and calculation of reflectance spectra, alongside the determination of taxonomic classification according to the Tholen and SMASSII systems, based on spectral morphology and selected spectral characteristics, were conducted for a sample of 19 asteroids, primarily consisting of Main Belt members (14). A comparison was made with the spectra of asteroids based on INASAN observations in 2013–2017 and the reflectivity spectra of asteroids obtained from Gaia (DR 3) observations, and their taxonomic types were determined without taking into account the albedo of the asteroids.*

Keywords: spectrophotometry, asteroids; reflectance spectra; Gaia DR3

1. Introduction

Asteroids are the least altered relics of the primordial matter of the Solar System. The study of the physical and chemical composition of these bodies is necessary for solving cosmogonic problems: analysis of the type of minerals that make up the surface of asteroids allows us to assess the plausibility of various models of the formation of the Solar System. In addition, asteroids are considered as possible sources of extraterrestrial natural resources (Board S. S. et al., 2010) [1].

The presence of fragmented material on the surface of asteroids allows us to determine their shape, structure, particle parameters, and also makes it possible to study their chemical and mineral composition. Traditional methods of studying these bodies are photometry, spectrophotometry, and polarimetry, which are independent and complement each other. Photometry and polarimetry are most effective in studying the physical parameters of solid celestial bodies, while spectrophotometry allows us to carry out a qualitative, and sometimes quantitative, assessment of the composition of the substance of these bodies. Spectrophotometry allows us to obtain a reflectivity spectrum of the entire visible hemisphere of a sufficiently distant celestial body, observed as a point-source object.

The spectral range of optical transparency of the Earth's atmosphere is approximately between 350 and 1000 nm. In this range, the asteroid only reflects solar radiation, so such a characteristic as "reflection spectrum" is used, which is the measured spectrum of the object divided by the average spectrum of the Sun. Spectral and geochemical studies of meteorites, which are most likely fragments of asteroids, show that the features of the reflection spectra in the range of ~200–2500 nm characterize their chemistry and mineralogy. That is, the asteroid's reflection spectrum (normalized to flux at wavelength of 550 nm) mainly characterizes the composition of the asteroid's matter. Bodies are categorized into several classes based upon the predominant substances within their composition.

2. Characteristics for the classification of the asteroids under study

C-type asteroids are important objects for studying the evolution of the Solar System and potential targets for future resource mining missions. Their composition allows us to study the early stages of planet formation and the possible presence of water. Research by Binzel (2019) [2] highlights the key role of these asteroids in understanding the evolution of the Solar System due to their pristine chemical composition. DeMeo and Carry (2014) [3] note the importance of spectral analysis for understanding the distribution of carbonaceous materials in the asteroid belt, showing that such asteroids may contain significant reserves of water in the form of hydrated minerals. Clark et al. (2002) [4] investigated the space weathering processes affecting the spectral properties of these objects and found that long-term exposure to the solar wind and micrometeoroid bombardment alters their surface properties, reducing reflectivity and changing spectral lines. Examples of this asteroid class include 51 Nemausa, 70 Panopaea, 107 Camilla, 144 Vibilia, 163 Erigone, 345 Tercidina, and 481 Emita.

M-class asteroids have been studied rather poorly and are classified as a separate class because their spectra in the 0.3-2.5 μm range do not have noticeable absorption bands, and their reflectivity increases with wavelength similar to the spectra of iron meteorites and enstatite chondrites with a high content of free metal (Lupishko et al., 2000) [5]. According to Tholen's spectral classification the (97) Klotho and (55) Pandora belongs to the metal-rich M-class asteroids, but radar observations do not confirm a notable content of iron-nickel composites in the composition of its surface (Shepard et al., 2005) [6]. It should be noted that asteroids of this type can vary significantly in their composition, ranging from metal-rich to metal-poor, and include various groups of minerals. In particular, Hardersen et al. (2011) [7] found diagnostic absorption bands of pyroxenes, olivines, phyllosilicates and hydroxides in the near infrared (NIR: ca. 0.75–2.50 μm) spectrum of 60% of Tholen class M/X asteroids. These data highlight the spectral and mineralogical diversity in the M-class asteroid population. Possible meteoritic analogues include mesosiderites, CB/CH chondrites and silicate-containing nickel-iron meteorites. Asteroids lacking characteristic spectral signatures are related to meteoritic analogues such as nickel-iron meteorites, enstatite chondrites and stony-iron meteorites.

S-type asteroids are silicate asteroids, which make up about 17% of all discovered asteroids. The concentration of celestial bodies in this class decreases with distance from the Sun. Asteroids of this class are moderately bright, with a slightly reddish color. Spectrophotometry indicates olivine, pyroxenes, and Fe-Ni metal (Lupishko et al., 2000) [5] as the main components of the S-type asteroids. Given that the majority of S-type asteroids exhibit an olivine-metal composition with a comparatively limited amount of pyroxene, it is postulated that contemporary S-type asteroids, such as (482) Petrina, are remnants of larger S-type asteroids that underwent fragmentation. These ancestral asteroids are theorized to have originated in the proximity of the core-mantle boundary within their respective parent bodies.

P-type asteroids are objects with a fairly low albedo of 0.02 to 0.07 and a flat reddish spectrum without noticeable absorption lines. Such properties are characteristic of carbon- or organic-enriched matter silicates that have not undergone significant changes since their formation (De Pater, Imke et al., 2001) [8], (Ehrenfreund et al., 2004) [9]. They are, for example, part of interplanetary dust, which probably filled the near-solar protoplanetary disk even before the formation of the planets. Based on this similarity, it can be assumed that P-asteroids are the most ancient, little-changed bodies in the Main Belt (McSween Jr. and Harry Y., 1999) [10]. Such asteroids may be rich in carbon and silicates, possibly mixed with water ice. According to the Malkhe classification, this class of asteroids includes (65) Cybele, (447) Valentine and (160) Una.

B-type asteroids are a relatively rare class of asteroids that belong to the carbonaceous asteroids and are predominantly found in the outer part of the Main Belt. They are generally similar to C-type asteroids, but are distinguished by an almost complete absence of absorption at wavelengths below 0.5 μm and have a slightly bluish color. Spectroscopic studies have suggested that the main components of the surface are anhydrous silicates, hydrated clay minerals, organic polymers, magnesites, and sulfides. Most asteroids that have signs of cometary activity belong to this class, for example, according to the SMASSII classification, asteroids (88) Thisbe and (47) Aglaja belong to this class.

X-type asteroids are a class of asteroids that cannot be classified into any of the other classes. Typically, such objects are assigned to M, E, or P classes after albedo analysis.

3. Statement of the research objective

It is known that the reflectivity spectra of asteroids observed with different detectors and at different epochs often show significant differences, mainly in the slope of the spectrum from blue to red wavelengths.

Reflectivity spectra of asteroids observed with different detectors and at various periods of time often show significant differences. This issue is the subject of an extensive analysis of the diversity of reflectivity spectra obtained at different epochs for moderately large and bright Main Belt asteroids. Mostly, such differences concern the slope of the spectrum from “blue” to “red” wavelengths. Sometimes such differences are considered to be a consequence of surface inhomogeneity, but this interpretation is often speculative.

The differences in the reflectivity spectra obtained may be related to the spectral variability of the asteroids and their heterogeneous composition, and to the fact that the comparison spectrum is not the spectrum of an ideal solar analogue. Research conducted over decades shows that there are essentially three physical processes that play a major role in the evolution of the asteroid population and affect the change in the reflectivity spectrum. The first is collisional evolution, which gradually affects the size distribution of Main Belt asteroids and their surfaces. When objects collide, the outer layers of the surfaces can be destroyed and fragmented, the inner layers of the asteroid can be exposed, changing the visible chemical composition of its surface. In addition, collisions can lead to an exchange of matter between the asteroid and the object it collided with. If the impactor and target asteroid initially belonged to different spectral classes and had different mineralogical compositions, then their collision leads to a mixing of materials. This makes it difficult to determine their spectral class, since the surface begins to show signs of different minerals characteristic of both parent bodies. The second is space weathering, which occurs due to cosmic rays, solar wind and collisions with micrometeoroids on the asteroid surface. Over decades, space weathering gradually changes the reflectance spectra of asteroids. The surface of the asteroid darkens and becomes reddish. This change is associated with processes that change the spectral characteristics of the surface, such as the formation of thin metallic films and a change in the size of regolith particles. The most important effects were found for the class of asteroids belonging to the S-class. This class includes objects considered to be the parent bodies of the most common class of meteorites - ordinary chondrites. The third is that a simple cycle of thermal expansion and contraction of the material constituting the outer layer of the surface regolith, due to the rotation of the asteroid, leads to a progressive evolution of the structural and thermal properties of the regolith.

Observations and analyses of reflectance spectra are essential for elucidating the principal physical mechanisms governing asteroid evolution and spectral alterations. Notably, there has been an increasing discovery of asteroids exhibiting sublimation-dust and dust activity triggered by diverse physical factors in recent years. This paper presents the findings of spectrophotometric observations conducted on several Main Belt primitive asteroids, aimed at detecting potential indications of sublimation-dust activity induced by elevated subsolar temperatures and solar eruptive events. This endeavor necessitates a comparative analysis of reflectance spectra derived from various sources and observational epochs. As an illustration, Busarev et al. (2019) posit that spectral signatures of sublimation activity are discernible in (51) Nemausa and (65) Cybele.

.

In the present study, one of the primary objectives is the selection of the most optimal stars—solar analogues—for accurate computation of asteroid reflectance spectra. The most common methodology for obtaining normalized asteroid reflectance spectra involves using a single solar analogue for each observed object, which is observed on the same night as the target. In contrast, this work employs a method of averaging the spectra of several top-quality solar analogues (described in detail in Section 3), which enhances the accuracy and reliability of the resulting spectra and prevents loss of observational data due to a poor choice of solar analogue. By comparing these results with data from other observatories, one can objectively assess the applicability and advantages of this approach based on the quality of the reflectance spectra.

4. Observations

To analyze the reflectivity spectra of individual Main Belt asteroids, data were obtained from three sources: observations conducted at different times at the Fesenkov Astrophysical Institute (FAI), the Institute of Astronomy of the Russian Academy of Sciences (INASAN), and the Gaia DR3 Mission of the European Space Agency (ESA).

The observations FAI were carried out in 2023 at the Assy-Turgen Observatory using a long-slit spectrograph based on volume-phase holographic gratings (VPHG) installed at the prime focus of the AZT-20 telescope with an aperture of 1.5 meters and a relative focal length of 5.72 meters (f=1:3.8). The focal lengths of the collimator and the spectrograph camera are 130 mm and 85 mm, respectively. The spectrograph is equipped with an iXon Ultra 888 EMCCD with a size of 1024 × 1024 pixels, and the pixel size is 13 microns, which gives an image scale of 0″.717 per pixel.

The observations were carried out in the low-resolution mode (R=600) using a grating of 360 lines per mm, a dispersion of 4.25 Å per pixel, in the first binning in the EMCCD mode with a gain of 5 and an exposure time of 10 seconds, the slit width of 9 arc seconds. To calibrate the wavelengths, the spectra of a standard source - a He-Ne-Ar lamp - were taken. The spectrum of the asteroids was obtained using the differential method - by comparing the fluxes from the object and a standard star. Solar analogues stars (class G stars) were used as standards.

Table 1 presents the designation of asteroid, date and time of observation, exposure time and air mass. Data format: 1 - Date and time in YYMMDD, 2 - Universal Time in hhmmss, 3 and 4 - right ascension and declination at the time of observation in the J2000, 5 - distance from the observer to the object (in AU), 6 - distance from the Sun to the object (in AU), 7 - solar elongation (in °), 8 - phase angle of the object (in °), 9 - predicted stellar magnitude, 10 - air mass, 11 - exposure time. Columns 3-9 are given according to the Minor Planet Center at the time of observations. The last row of the table contains information on the EMCCD mode used during observations.

INASAN reflectivity spectra were obtained at the Peak Terskol observatory (3150 meters above sea level) using a 2-meter telescope manufactured by Carl Zeiss Jena GmbH, with a prism CCD spectrometer (WI CCD 1240×1150). Low-resolution spectra (R≈100) were used in INASAN observations, which nevertheless allowed determining the spectral classes of asteroids and identifying large features of the reflectivity spectra (wide absorption bands). Data processing was performed using DECH software (DECH20T and DECH95 packages).

The GAIA mission of the European Space Agency has been regularly observing Solar System objects since the beginning of its operations in August 2014. The third Gaia data release (DR3) includes for the first time the mean reflectance spectra of a selected sample of 60,518 such objects, mostly asteroids, observed between 5 August 2014 and 28 May 2017. Each reflectance spectrum was obtained from measurements taken with the “blue” and “red” photometers operating in the wavelength ranges 330–680 nm and 640–1050 nm, respectively (Gaia Collaboration: L. Galluccio et al., 2023) [12]. The Gaia DR3 database presents the mean reflectance spectrum for each asteroid, calculated for 16 points representing integrated reflectivity.

5. Research methodology

The main research method is the meticulously carried out observations and analysis of the spectra of solar radiation reflected by the object and the spectra of solar-type stars. Data processing was performed using standard procedures, using the Image Reduction and Analysis Facility (IRAF) package. The spectra of asteroids and the standard source were processed using an identical technique, taking into account the effect of air mass changes during observations.

Observational and instrumental difficulties in observing asteroids in the range below 5000Å make this wavelength range poorly studied compared to the visible and near infrared range. In particular, the choice of the solar analog star used to obtain the asteroid reflectivity spectrum is a major challenge (Noem et al., 2016) [13], (Cellino et al., 2020) [14], (de León et al., 2010) [15].

Not all solar analogues present in catalogues are truly identical to the Sun. This effect is particularly important in the blue part of the spectrum, where solar analogues often show significant differences with respect to each other and to the solar spectrum (Raḿırez et al., 2012) [16]. Furthermore, the suitability of many used solar analogues is usually assessed only in the visible wavelength range, while some of these objects show spectra that are quite different from the Sun's spectrum at wavelengths below 5500Å. The stars HD 28099 (Hyades 64) and HD 186427 (16 Cyg B) are well-studied solar analogues that have spectra very similar to the Sun's spectrum in the wavelength range between 3600Å and 5500Å.

In Tinaut-Ruano et al. (2023) [17], the authors assessed the suitability of the solar analogues selected for the near-ultraviolet reflectivity study of asteroids included in the Gaia DR3 release. They found that the solar analogues selected for Gaia DR3 to calculate the asteroid reflectivity spectra have a systematically redder spectral tilt at wavelengths shorter than 5500Å than Hyades 64.

For the analysis of asteroid reflectivity spectra, it is important to select comparison stars whose spectral type is as close as possible to the Sun's. Additional criteria are availability of the star for observations on a given night, as well as its sufficient brightness to obtain a spectrum with a high signal-to-noise ratio. To minimize possible errors when using the spectra of Sun-like stars to obtain reflectivity spectra, the spectra of several best (in terms of the quality of the obtained spectra and proximity to the Sun’s spectral type) Sun-like stars observed on the night of observations were averaged, as was done by Farnham et al. (2000) [18] and Tedesco et al. (1982) [19]. Four stars were selected from a total of 12 observed stars. An analysis was performed of the extinction-corrected and 0.55 μm flux-normalized spectra of all standard spectra observed on that night. Figure 1 shows the normalized spectra of the standard stars selected for analysis - HD 34411 (G1.5IV), HD 13043 (G2V), HD 219018 (G5V). Then, the average spectrum of the best solar-like stars for the given night was compiled, which is shown in the figure as the “average spectrum”.

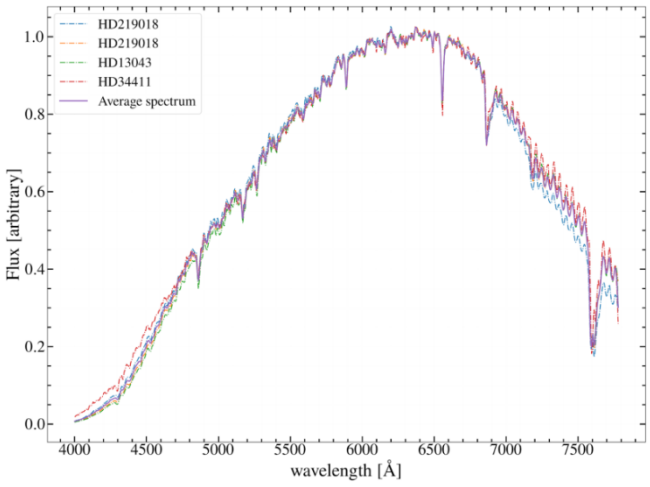

Fig.1. - Normalized spectra of standard stars - HD 34411 (G1.5IV), HD 13043 (G2V), HD 219018 (G5V)

The resulting reflectivity spectra of asteroids were obtained by dividing the asteroid spectrum by the spectrum of a standard star, in our case by the same averaged spectrum of several standard stars. This procedure introduces additional noise into the final result due to the presence of noise in the spectra of solar analog stars.

Our experience with satellite reflectance spectra has shown that the Butterworth filter (Serebryanskiy et al., (2022)) [20] is effective for smoothing the reflectance spectra. The Butterworth filter is implemented in the *scipy* package (Virtanen et al., 2020) [21] using the *signal.butter* method, which uses the order of the filter and cutoff frequency in Nyquist frequency units as parameters. In our case, the filter's order is chosen to be 3, and the cutoff frequency is 0.086, which corresponds to smoothing the spectrum in a window of 50Å wide with a spectral resolution of about 4Å. Testing with different cutoff frequency values showed that this is the optimal value and the smoothing result, when choosing this parameter in a reasonable range, does not change the final conclusions. The smoothing process itself is carried out by the *signal.fultfilt* method of the *scipy* package. Measurement errors in the reflection spectra were determined through averaging multiple spectra to account for fluctuations in observational conditions, rather than solely relying on the formal errors of the spectra or the signal-to-noise ratio. The final error, incorporating the smoothing procedure, is within 10% of the reflection value. Notably, a substantial increase in error below a 4000Å wavelength range imposes limitations on the analyzed spectral range.

6. Results and discussion

A comparative analysis of the reflectance spectra obtained at FAI in 2023 was carried out with the spectra obtained at INASAN in 2013-2017 and with the reflectance spectra from the GAIA DR3 database. Figure 2 shows the reflectivity spectra of asteroids (51) Nemausa, (70) Panopaea, (107) Camilla, 144 Vibilia, 163 Erigone, 345 Tercidina, 481 Emita, which according to the classification of Tholen D.J. (1989) [22] belong to class C, as well as asteroids (366) Vincentina, (381) Myrrha, (407) Arachne, which belong to subclass Ch (SMASSII classification). The results obtained align broadly with those from independent sources. Reflectance spectra of (51) Nemausa, (366) Vincentina, (407) Arachne, (481) Emita, and (107) Camilla demonstrate qualitative correspondence to the INASAN spectra, exhibiting a variation in the gradient within the blue region, and deviate from the GAIA spectra. The observed spectral discrepancy in the 0.4-0.6 nm range may indicate a subtle manifestation of sublimation activity.

Figure 3 shows the reflectivity spectra of the asteroids (97) Klotho and (55) Pandora, according to the classification of Tholen. Whilst for the asteroid (97) Klotho we obtained a fairly good agreement with the INASAN and GAIA DR3 data during the comparative analysis, the spectrum of (55) Pandora does not agree with either the INASAN or GAIA data. At the same time, the INASAN and GAIA DR3 data agree well in the spectral region of 5000-9500Å. According to the spectral classification of Tholen, the asteroid (55) Pandora belongs to class M, but according to the SMASS classification it belongs to class X. Rather, it corresponds to the spectral classification of SMASS (class X), showing stronger absorption in the region below 0.5 μm.

Asteroid (482) Petrina (Fig.4) belongs to the Tholen class S and has growth in the long-wavelength region and, according to Shcherbina et al. (2019) [23], corresponds to high-temperature mineralogy. According to FAI data, the reflectivity spectrum also increases in the long-wavelength region and is closer to the GAIA DR3 data. This asteroid has a high albedo (0.24), which indirectly confirms its belonging to the S class.

Fig.5 shows the reflectivity spectra of class P asteroids - (65) Cybele, (447) Valentine and (160) Una. The reflectivity spectrum of the asteroid (65) Cybele shows agreement with the GAIA DR3 spectrum obtained for this class and has discrepancies with the spectrum obtained by INASAN in 2017 (Fig.5). However, the peculiarity of the reflectivity spectrum obtained at the Peak Terskol observatory, namely the maximum reflectivity in a fairly wide range of 0.4 to 0.7 μm, changing in intensity in the range of 0.4 to 0.5 μm, was explained in Busarev et al. (2019) [11] by the presence of weak sublimation activity of the asteroid. The sharp change in the shape of the reflectivity spectrum in the short-wave region according to FAI data for (160) Una and the slight increase in the reflectivity spectrum according to INASAN data remain questionable and require additional observations of this asteroid.

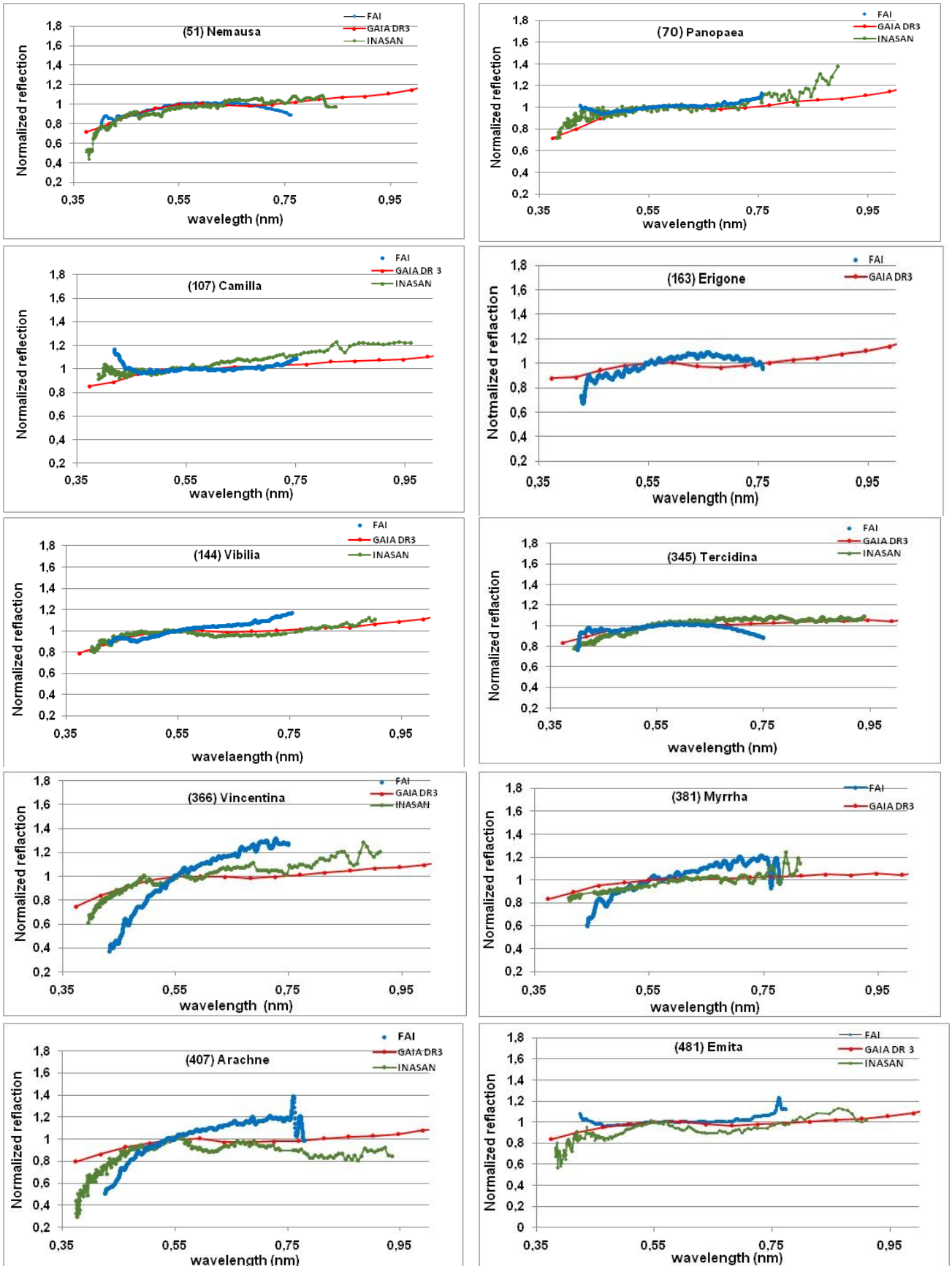

Fig.2. Reflectivity spectra of class C and subclass Ch asteroids

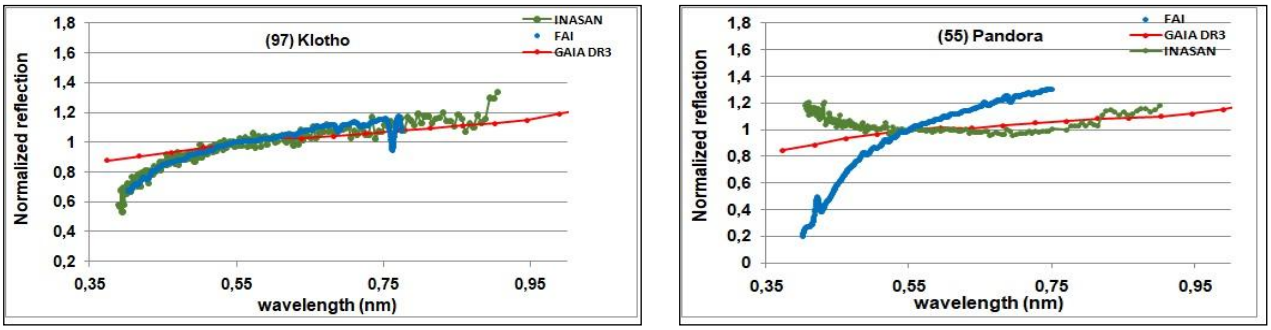

Fig. 3. Reflectivity spectra of asteroids (97) Klotho and (55) Pandora of class M

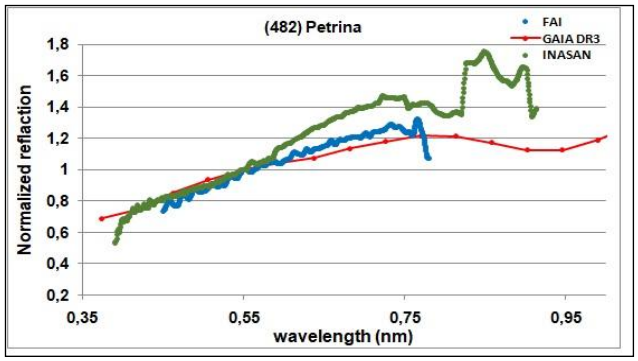

Fig.4. Reflectivity spectrum of the S-type asteroid (482) Petrina

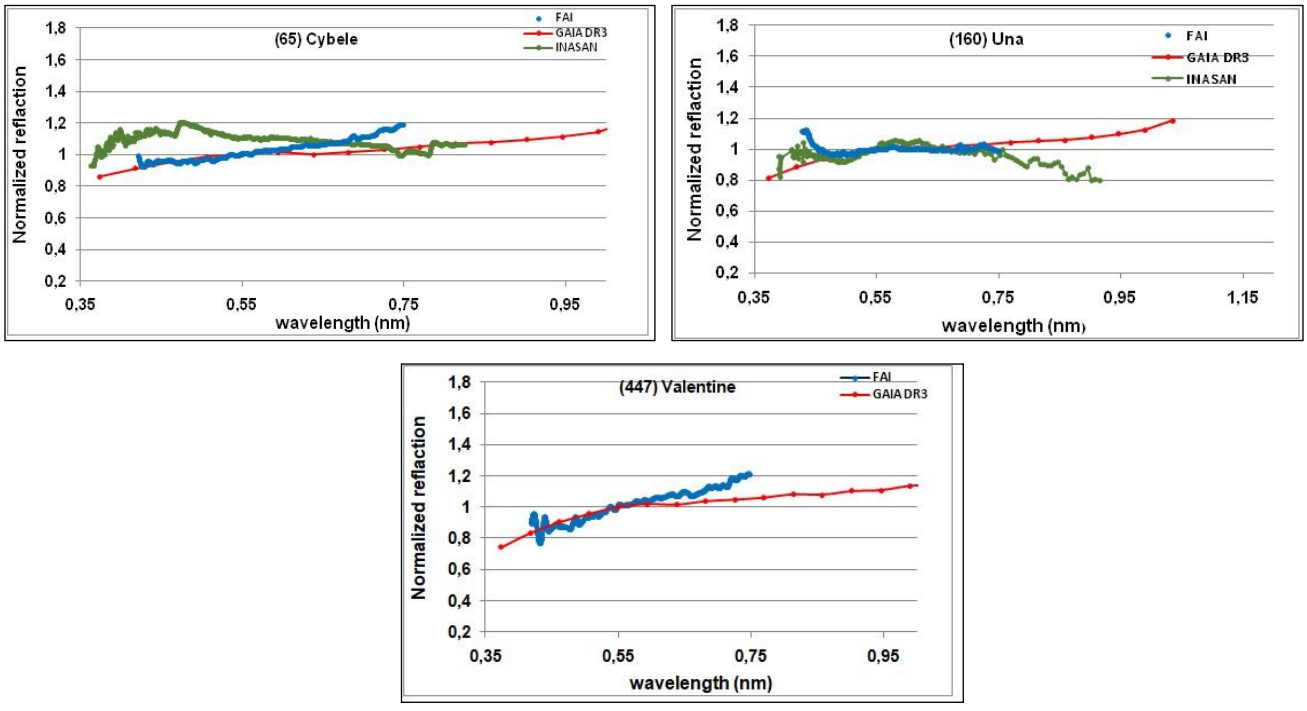

Fig.5. Reflectivity spectra of asteroids (65) Cybele, (447) Valentine and (160) Una

Fig.6 shows the reflectivity spectra of asteroids (88) Thisbe и (47) Aglaja. (88) Thisbe is a Main Belt asteroid of SMASSII class B, Tholen class CF, and Malkhe class C, indicating that it likely contains hydrogen, nitrogen, ammonia, and iron. (47) Aglaja is Tholen class C and has a

carbonaceous composition. The SMASSII classification system rates it as a rare B-class asteroid associated with the presence of magnetite, which gives the asteroid a blue color. The reflectivity spectrum of asteroid (47) Aglaja shows good agreement with the GAIA DR3 spectrum and the spectrum obtained by INASAN in 2017. The reflectivity spectrum of asteroid (88) Thisbe has discrepancies with the spectrum obtained by INASAN in 2017 and the spectrum of the GAIA DR3 database. We suspect the presence of sublimation activity. To clarify the observed variations in the short wavelength region of asteroid (88) Thisbe's reflectance spectrum, additional observations at different heliocentric distances, including around perihelion, are required. The spectral classification derived from our measurements is consistent with that reported by previous studies. Consequently, asteroid (88) Thisbe should be considered a promising candidate for activity and included in future observation programs.

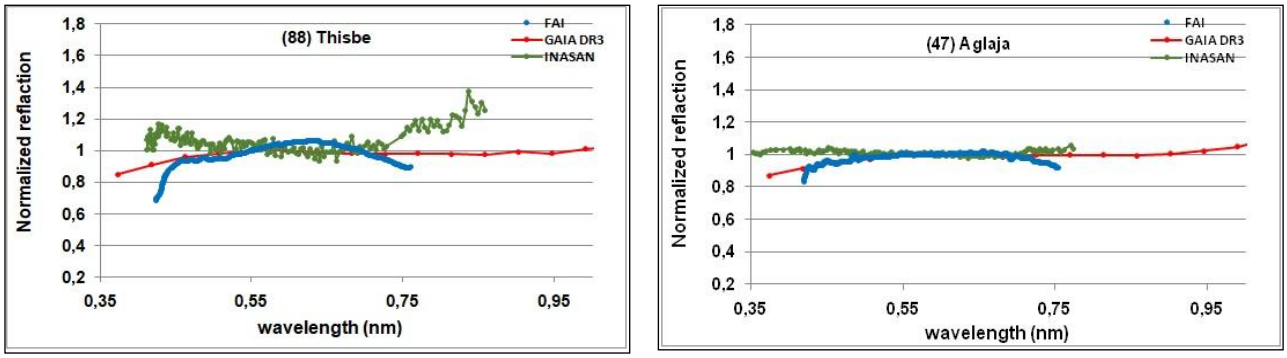

Fig.6. Reflectivity spectra of asteroids (88) Thisbe and (47) Aglaja

Fig.7 shows the reflectivity spectra of (718) Erida, which, according to SMASSII, belongs to class X, i.e. to asteroids that remain poorly classified. A more precise determination of the asteroid class requires additional albedo analysis and comparison with classes C, S and M.

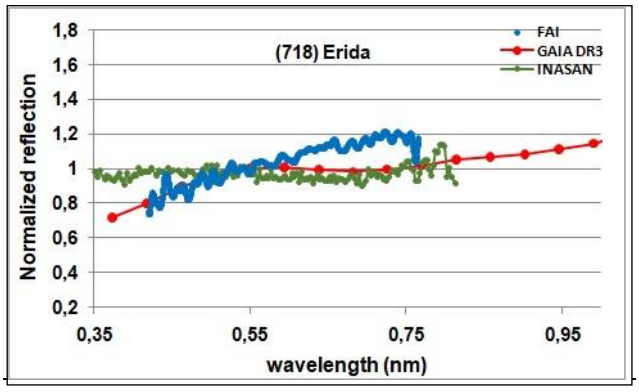

Fig.7. Reflectivity spectra of asteroids (718)

7. Conclusions

Spectral processing and reflectance spectra calculations were performed for 19 Main Belt asteroids, followed by taxonomic classification according to Tholen and SMASSII based on spectral morphology and characteristic features. Reflectance spectra were derived from data collected at the Fesenkov Astrophysical Institute (FAI), the Institute of Astronomy of the Russian Academy of Sciences (INASAN), and the Gaia DR3 Mission of the European Space Agency (ESA). To mitigate potential inaccuracies in reflectance spectra resulting from the use of solar-analog stars, multiple high-quality solar-analog star spectra, closely matching

.

the Sun's spectral class and obtained during the observation period, were averaged. Furthermore, to minimize noise in the reflectance spectra, multiple spectra were averaged to account for observational variations.

This approach delivers high-quality reflectance spectra comparable to those obtained using a single standard star analogue. Moreover, it minimizes the risk of unwanted spectral distortions—spurious features in the asteroid's reflectance spectrum caused by employing an improperly matched solar analogue that significantly differs from the Sun.

The study's findings indicate that the reflection spectra of asteroids (51) Nemausa, (366) Vincentina, (407) Arachne, (481) Emita, and (107) Camilla exhibit qualitative correspondence with the INASAN spectra. This correspondence is characterized by a variation in gradient within the blue spectral region, and these spectra are notably divergent from the GAIA spectra. It is posited that the spectral disparity observed within the 0.4-0.6 nm range may signify a subtle expression of sublimation activity.

The discrepancy observed between the FAI and INASAN data regarding the reflectivity spectrum of asteroid (160) Una, specifically the sharp alteration in the short-wave region and the marginal increase, respectively, warrants further investigation and additional observational data for confirmation.

The reflectivity spectrum of asteroid (718) Erida, which belongs to the SMASSII class X and was obtained by FAI, does not permit the precise classification of the asteroid. Furthermore, evidence confirms the potential sublimation activity of asteroids (51) Nemausa and (65) Cybele.

To ascertain the taxonomic classification of individual asteroids from spectra acquired by FAI, supplementary investigations will be conducted employing the "template" methodology delineated in the study by Savelov et al. (2022) [24], alongside the utilization of visual albedo, a parameter indicative of the chemical and mineralogical attributes of the asteroids' surface material.

Conflict of interest statement.
The authors declare that they have no conflict of interest in relation to this research, whether financial, personal, authorship or otherwise, that could affect the research and its results presented in this paper

CRediTauthor statement
Aimanova G.K. and Serebryanskiy A.V.: Conceptualization, Methodology, Investigation, Data Curation, Writing Original Draft; Shcherbina M.P.: Methodology, Resources, Validation; Krugov M.A.: Investigation, Resources.
The final manuscript was read and approved by all authors.

Funding

This research has been funded by Program No. BR20381077 of the Aerospace Committee of the Ministry of Digital Development, Innovations and Aerospace Industry of the Republic of Kazakhstan.

The observations at the "Peak Terskol" Observatory were conducted as part of the state assignment of the Institute of Astronomy of the Russian Academy of Sciences, code FFWN-2024-0010, approved by the Ministry of Education and Science of Russia, using the Large-Scale Research Facility "Zeiss-2000 Telescope" of the Core Shared Research Facilities "Terskol Observatory" of INASAN.

Acknowledgements

We thank the FAI observers for their efficient work.

References

1 Board S.S. (2010) Defending Planet Earth: Near-Earth Object Surveys and Hazard Mitigation Strategies. National Academies Press, 152. https://doi.org/10.17226/12842

2 Binzel R.P. (2019) Small bodies looming large in planetary science. *Nature Astronomy*, 3(4), 282-283. https://doi.org/10.1038/s41550-019-0747-6

3 DeMeo F.E., Carry B. (2014) Solar System evolution from compositional mapping of the asteroid belt. *Nature, 505,* 629-634. https://doi.org/10.48550/arXiv.1408.2787

4 Clark B.E., Hapke B., Pieters C., Britt D. (2002) Asteroid Space Weathering and Regolith Evolution. *Asteroids III*, 585-599. Available at: https://www.researchgate.net/publication/253857329_Asteroid_Space_Weathering_and_Regolith_Evolution

5 Lupishko D., Karazin V.N. (2000) Physical properties of asteroids. *Astronomical School's Repor., 1(2).* 63-77. https://doi.org/10.18372/2411-6602.01.2063

6 Shepard M.K. (2005) A Long-Term Radar Survey of M-Class Asteroids. *Bulletin of the American Astronomical Society, 37.* 628. Available at: https://ui.adsabs.harvard.edu/abs/2005DPS....37.0707S/abstract

7 Hardersen P.S., Cloutis E.A., Reddy V., Mothe-Diniz T., Emery J.P. (2011). The M-/X-asteroid menagerie: Results of an NIR spectral survey of 45 main-belt asteroids. *Meteoritics & Planetary Science, 46(12)*. 1910-1938. https://doi.org/10.1111/j.1945-5100.2011.01304.x

8 De Pater, Imke; Lissauer, Jack Jonathan (2001). Planetary sciences. Cambridge University Press. 528. Available at: https://books.google.kz/books?id=RaJdy3_VINQC&printsec=frontcover&hl=ru&source=gbs_ge_summary_r&cad=0#v=onepage&q&f=false

9 Ehrenfreund P., Irvine W.M., Owen T., Becker L., Jen Blank, Brucato J.R., Colangeli L., Derenne S., Dutrey A., Despois D., Lazcano A., Robert F. (2004). *Astrobiology: Future Perspectives.* Springer Science & Business. 159. Available at: https://www.amazon.ae/Astrobiology-Future-Perspectives-P-Ehrenfreund/dp/1402023049

10 McSween Jr, Harry Y. (1999). *Meteorites and their Parent Planets*. Cambridge University Press. 324. Available at: https://www.amazon.com/Meteorites-Parent-Planets-Harry-McSween/dp/0521587514

11 Busarev V.V., Shcherbina M.P., Barabanov S.I., Irsmambetova T.R., Kokhirova G.I., Khamroev U.Kh., Khamitov I.M., Bikmaev I.F., Gumerov R.I., Irtuganov E.N. & Mel'nikov S.S. (2019) Confirmation of the Sublimation Activity of the Primitive Main-Belt Asteroids 779 Nina, 704 Interamnia, and 145 Adeona, as well as its Probable Spectral Signs on 51 Nemausa and 65 Cybele. *Solar System Research*, 53. 261-277. https://doi.org/10.1134/S0038094619040014

12 Gaia Collaboration: L. Galluccio, et al. (2023) Gaia Data Release 3: Reflectance spectra of Solar System small bodies. *A&A*, 674 (A35), 29. https://doi.org/10.1051/0004-6361/202243791]

13 Pinilla-Alonso, Noem, de Le´on, J., Walsh, K. J., Campins, H., Lorenzi, V., Delbo, M., DeMeo, F., Licandro, J., Landsman, Z., Lucas, M. P., Al´ı-Lagoa, V., Burt, B. (2016) Portrait of the Polana-Eulalia Family Complex: Surface homogeneity revealed from Near-Infrared Spectroscopy. *Icarus, 274:231-248.* https://doi.org/10.1016/j.icarus.2016.03.022

14 Cellino A., Ph. Bendjoya, M. Delbo, L. Galluccio, J. Gayon-Markt, P. Tanga, and E. F. Tedesco (2020) Ground-based visible spectroscopy of asteroids to support the development of an unsupervised Gaia asteroid taxonomy. *A&A,* 642. A80. https://doi.org/10.1051/0004-6361/202038246

15 de León, J. Licandro, M. Serra-Ricart, N. Pinilla-Alonso, H. Campins (2010) Observations, compositional, and physical characterization of near-Earth and Mars-crosser asteroids from a spectroscopic survey. *A&A,* 517. A23. https://doi.org/10.1051/0004-6361/200913852

16 Ramırez I, R. Michel, R. Sefako, M. Tucci Maia, W. J. Schuster, F. van Wyk, J. Melendez, L. Casagrande, and B. V. Castilho (2012). The UBV(RI) Colors of the Sun. *The Astrophysical Journal, 752, 5, 13.* https://doi.org/10.1088/0004-637X/752/1/5

17 Tedesco E.F., Tholen D.J., Zellner B. (1982) The eight-color asteroid survey - Standard stars. *AJ,* 87(11). 1585-1592. Available at: https://adsabs.harvard.edu/full/1982AJ.....87.1585T

18 Farnham T. L., Schleicher D. G., A'Hearn M. F. (2000) The HB Narrowband Comet Filters: Standard Stars and Calibrations. *Icarus, 147(1),* 180-204. https://doi.org/10.1006/icar.2000.6420

19 Tinaut-Ruano F., E. Tatsumi, P. Tanga, J. de León, M. Delbo, F. De Angeli, D. Morate , J. Licandro, and L. Galluccio (2023). Asteroids' reflectance from Gaia DR3: Artificial reddening at near-UV wavelengths. *A&A*, 669, L14. https://doi.org/10.1051/0004-6361/202245134]

20 Serebryanskiy A.V., Omarov Ch.T., Aimanova G.K., Krugov M.A., Akniyazov Ch.B. (2022). Spectral Observations of Geostationary Satellites. *Eurasian Physical Technical Journal, 19(2).* 93-100. https://doi.org/10.31489/2022No2/93-100

21 Virtanen P., Ralf Gommers, Travis E. Oliphant, Matt Haberland, Tyler Reddy, David Cournapeau, Evgeni Burovski, Pearu Peterson, Warren Weckesser, Jonathan Bright, Stéfan J. van der Walt, Matthew Brett, Joshua Wilson, K. Jarrod Millman, Nikolay Mayorov, etc., and SciPy 1.0 Contributors. (2020) SciPy 1.0: Fundamental Algorithms for Scientific Computing in Python. *Nature Methods, 17(3),* 261-272. https://doi.org/10.1038/s41592-019-0686-2

22 Tholen D.J. Asteroid taxonomic classifications. (1989) IN: Asteroids II; Proceedings of the Conference, Tucson, AZ, Mar. 8-11, 1988 (A90-27001 10-91). Tucson, AZ, University of Arizona Press, 1139-1150. Available at: https://ui.adsabs.harvard.edu/abs/1989aste.conf.1139T/abstract

23 Shcherbina M.P., Busarev V.V., Barabanov S.I. (2019) Spectrophotometric Studies of Near-Earth and Main-Belt Asteroids. *Moscow University Physics Bulletin, 74(6).* 675–678. Available at: https://link.springer.com/article/10.3103/ S0027134919060237

.

24 Savelova A.A., Busarev, V.V., Shcherbina, M.P., Barabanov, S.I. (2022) Using "templates" of spectral types of asteroids to enhance the mineralogy of these bodies and detect the signs of sublimation-pyretic and solar activity. *INASAN Science Reports*, 7, 143-148. http://dx.doi.org/10.51194/INASAN.2022.7.2.008 [in Russian]

AUTHORS' INFORMATION

Serebryanskiy, Alexander Vladimirovich — PhD, Head of Observational Astrophysics Department, Fesenkov Astrophysical Institute, Almaty, Kazakhstan; https://orcid.org/0000-0002-4313-7416; serebryanskiy@fai.kz

Aimanova, Gauhar Kopbaevna — Candidate of Physical and Mathematical Sciences, Chief Researcher, Fesenkov Astrophysical Institute, Almaty, Kazakhstan; https://orcid.org/0000-0002-3869-8913; gauhar@fai.kz

Shcherbina, Marina P. — Candidate of Physical and Mathematical Sciences, Researcher, Institute of Astronomy of the Russian Academy of Sciences; Sternberg Astronomical Institute, Moscow State University, Moscow, Russia; Scopus Author ID: 57210443798 57210443798; https://orcid.org/0000-0002-8455-2034; mpshcherbina@inasan.ru

Krugov, Maxim A. — Master, Engineer, Fesenkov Astrophysical Institute, Almaty, Kazakhstan; https://orcid.org/0000-0002-2788-2176; krugov@fai.kz

Appendix

Table1. Logs of observations

Date (y m d)	UT (h m s)	R.A. (h m s)	Decl. (° ‘ “)	Delta (AU)	R (AU)	Elong (°)	Ph (°)	$V^{(m)}$	Airmass	Exp Time (s)
1	2	3	4	5	6	7	8	9	10	11
47 Aglaja										
2023 11 03	151112	22 03 42.0	-13 22 29	2.067	2.549	107.7	21.8	12.9	1.907	120
2023 11 03	151316	22 03 42.0	-13 22 28	2.067	2.549	107.7	21.8	12.9	1.903	120
51 Nemausa										
2023 11 03	161256	22 54 59.7	-08 20 26	1.863	2.524	121.2	19.7	12.1	1.709	120
2023 11 03	161502	22 54 59.7	-08 20 27	1.863	2.524	121.2	19.7	12.1	1.715	120
55 Pandora										
2023 11 03	180255	23 31 11.7	-03 04 40	1.585	2.362	131.4	18.3	11.7	1.835	120
2023 11 03	180501	23 31 11.7	-03 04 40	1.585	2.362	131.4	18.3	11.7	1.849	120
65 Cybele										
2023 11 04	190303	04 20 35.2	+16 43 57	2.893	3.816	155.2	6.3	12.6	1.167	120
2023 11 04	190508	04 20 35.1	+16 43 57	2.893	3.816	155.2	6.3	12.6	1.165	120
70 Panopaea										
2023 11 04	192008	04 18 18.0	+24 39 53	1.811	2.740	154.6	8.9	12.3	1.077	240
2023 11 04	192412	04 18 17.9	+24 39 53	1.811	2.740	154.6	8.9	12.3	1.074	240
88 Thisbe										
2023 11 03	163654	23 17 42.7	+03 39 03	1.710	2.474	130.6	17.7	11.4	1.365	120
2023 11 03	163900	23 17 42.7	+03 39 03	1.710	2.474	130.6	17.7	11.4	1.369	120
97 Klotho										
2023 11 03	182443	23 33 56.5	-12 48 14	1.437	2.188	127.6	21.0	11.4	2.637	120
2023 11 03	182646	23 33 56.5	-12 48 14	1.437	2.188	127.6	21.0	11.4	2.667	120
107 Camilla										
2023 11 03	134138	21 08 37.4	-12 22 51	3.444	3.671	95.3	15.6	13.5	1.784	10
2023 11 03	134155	21 08 37.5	-12 22 51	3.444	3.671	95.3	15.6	13.5	1.784	10
2023 11 03	134226	21 08 37.5	-12 22 51	3.444	3.671	95.3	15.6	13.5	1.785	60
2023 11 03	134332	21 08 37.5	-12 22 51	3.444	3.671	95.3	15.6	13.5	1.787	60
2023 11 04	142703	21 09 08.6	-12 23 07	3.459	3.671	94.4	15.6	13.5	1.923	240
2023 11 04	143109	21 09 08.7	-12 23 07	3.459	3.671	94.4	15.6	13.5	1.924	240
144 Vibilia										
2023-11-04	171606	03 40 24.6	+15 28 22	1.144	2.117	164.7	7.1	10.6	1.331	120
2023-11-04	171812	03 40 24.5	+15 28 22	1.144	2.117	164.7	7.1	10.6	1.324	120
160 Una										
2023-11-04	194708	05 23 25.3	+28 03 24	1.711	2.549	139.6	14.6	13.1	1.097	240
2023-11-04	195158	05 23 25.2	+28 03 24	1.711	2.549	139.7	14.6	13.1	1.090	240

.

Continuation of the Table 1.

1	2	3	4	5	6	7	8	9	10	11
163 Erigone										
2023-11-03	153139	22 15 17.9	-12 26 30	1.857	2.393	110.6	22.8	14.1	1.887	120
2023-11-03	153343	22 15 17.9	-12 26 30	1.857	2.393	110.6	22.8	14.1	1.895	120
345 Tercidina										
2023 11 03	184719	00 30 23.9	+06 21 15	1.341	2.248	148.6	13.3	12.3	1.468	120
2023 11 03	184923	00 30 23.9	+06 21 14	1.341	2.248	148.6	13.3	12.3	1.476	120
366 Vincentina										
2023 11 03	155150	22 33 43.9	-07 04 42	2.411	2.992	116.8	17.2	13.9	1.661	120
2023 11 03	155356	22 33 43.9	-07 04 421	2.411	2.992	116.8	17.2	13.9	1.667	120
381 Myrrha										
2023 11 03	174225	23 24 42.2	-17 57 06	2.552	3.202	123.0	15.1	13.8	2.715	120
2023 11 03	174429	23 24 42.1	-17 57 06	2.552	3.202	123.0	15.1	13.8	2.741	120
407 Arachne										
2023 11 21	162505	05 54 52.6	+30 29 09	1.627	2.526	149.1	11.6	13.0	1.640	240
2023 11 21	162913	05 54 52.4	+30 29 09	1.627	2.526	149.1	11.6	13.0	1.613	240
447 Valentine										
2023 11 03	165015	02 35 55.0	+11 13 12	1.862	2.853	176.1	1.3	12.9	1.291	120
2023 11 03	165221	02 35 55.9	+11 13 12	1.862	2.853	176.1	1.3	12.9	1.287	
481 Emita										
2023 11 03	184257	04 04 38.4	+16 48 19	1.358	2.308	158.0	9.3	11.9	1.173	120
2023 11 03	184502	04 04 38.3	+16 48 19	1.358	2.308	158.0	9.3	11.9	1.170	120
482 Petrina										
2023 11 03	144726	21 57 53.3	-08 33 51	2.458	2.921	108.0	18.9	14.2	1.652	120
2023 11 03	144931	21 57 53.3	-08 33 51	2.458	2.921	108.0	18.9	14.2	1.656	
718 Erida										
2023 11 03	171341	23 24 44.0	-09 30 56	2.837	3.527	127.3	12.9	15.5	1.885	240
2023 11 03	171747	23 24 44.0	-09 30 56	2.837	3.527	127.3	12.9	15.5	1.906	240
TEMP = - 60 (matrix cooling temperature); READTIME = 1.0E-06 (Pixel readout time); GAIN=5 (signal gain factor)										